


## Article

# Highly Selective Catalytic Properties of HZSM-5 Zeolite in the Synthesis of Acetyl Triethyl Citrate by the Acetylation of Triethyl Citrate with Acetic Anhydride

Kyong-Hwan Chung <sup>1</sup>, Sangmin Jeong <sup>1</sup>, Hangun Kim <sup>2</sup>, Sun-Jae Kim <sup>3</sup> , Young-Kwon Park <sup>4</sup> and Sang-Chul Jung <sup>1,\*</sup>

<sup>1</sup> Department of Environmental Engineering, Sunchon National University, 255 Jungang-ro, Sunchon, Jeonnam 57922, Korea; likeu21@naver.com (K.-H.C.); y1b2b5@naver.com (S.J.)

<sup>2</sup> College of Pharmacy, Sunchon National University, 255 Jungang-ro, Sunchon, Jeonnam 57922, Korea; hangunkim@sunchon.ac.kr

<sup>3</sup> Faculty of Nanotechnology and Advanced Materials Engineering, Sejong University, 209 Neungdong-ro, Gwangjin-gu, Seoul 05006, Korea; sjkim1@sejong.ac.kr

<sup>4</sup> School of Environmental Engineering, University of Seoul, 163 Seoulsiripdaero, Dongdaemun-gu, Seoul 02504, Korea; catalica@uos.ac.kr

\* Correspondence: jcs@sunchon.ac.kr; Tel.: +82-61-750-3814

Received: 30 September 2017; Accepted: 26 October 2017; Published: 30 October 2017

**Abstract:** The catalytic activities of acid catalysts for the acetylation of triethyl citrate with acetic anhydride in the preparation of acetyl triethyl citrate were evaluated. Microporous zeolites such as HZSM-5 and HY zeolites catalysts were introduced as heterogeneous acid catalysts. HZSM-5 zeolite catalysts showed a high conversion of triethyl citrate and excellent selectivity of acetyl triethyl citrate. The catalytic activities of HZSM-5 zeolites were superior to those of the HY zeolites. In particular, the selectivity of acetyl triethyl citrate on HZSM-5 zeolites exceeded 95%. The moderate acid strength of HZSM-5 (Si/Al = 75) zeolite led to the highest catalytic activities among the HZSM-5 zeolite catalysts, which have various acid strengths.

**Keywords:** acetyl triethyl citrate; HZSM-5 zeolite; acetylation; triethyl citrate; plasticizer

## 1. Introduction

Polyvinyl chloride (PVC) is one of the useful and important polymers that is used widely in the formation of rigid and flexible PVC [1,2]. Plasticizers are added to PVC in the production of flexible PVC. Phthalic esters, such as di-2-ethylhexyl phthalate, diisodecyl phthalate, and diisononyl phthalate, have been used as plasticizers. On the other hand, phthalic esters are toxic and in some instances have been included in legislation outlining harmful materials [3,4]. Therefore, phthalate plasticizers are restricted for use in toys for toddlers, and their use will be limited further in future human sensitive applications, such as food packaging and medical tools.

Although phthalates are well-known general-purpose plasticizing agents that have been used in a variety of polymeric materials [5–7], some studies have indicated that they may represent certain risks to human health and are not biodegraded easily [8–12]. Furthermore, in traditional phthalic anhydride synthesis processes from the gas-phase oxidation of naphthalene, some aromatic trace impurities may remain in the plasticizer, preventing its use in products designed for direct contact with humans [13]. In contrast, despite biobased plasticizers, such as citric acid esters (with or without acetylation), not being for general purpose, they are generally recognized as safe (GRAS) by different international

regulatory agencies. This characteristic makes citrates suitable plasticizers for pharmaceutical and cosmetic applications, medical devices, food packaging, and toys [14,15].

Among the variety of citrate esters, tri-1-butyl citrate (TBC) is a widely used constituent in cosmetic products and as a raw material to produce acetyl tri-1-butyl citrate (ATBC). Acetylated tributyl citrate provides even better results as a plasticizing agent for PVC [16]. It has been known the method for TBC production using a homogeneous acid catalyst in the batch reaction system [17–19]. Some studies have also reported that the ion exchange resins as heterogeneous catalysts present the benefit of avoiding the need for corrosion-resistant materials [20]. The homogeneous catalysts are very corrosive to equipment and are difficult to remove. However, the heterogeneous catalysts are preferred because they are more active and efficient in reaching high conversions to the trialkyl ester below the decomposition temperature of citric acid ( $\sim 175\text{ }^{\circ}\text{C}$ ) [21]. The reaction conditions reported in previous reports are summarized as 8:1 to 16:1 of initial reactants molar ratio, 363–393 K of reaction temperature, and 0.5–1.5 wt % of catalyst loading [22].

Acetyl triethyl citrate (ATEC) is an ester derived from citric acid, which can be used as a green and nontoxic plasticizer to replace phthalate esters in many plastic products, such as toys, child care articles, food packages, and medicinal instruments [23–26]. ATEC seems to be too polar for PVC. ATEC is already known as a commercial product, i.e., Citroflex<sup>®</sup> A-2, which is used with cellulosic derivatives, as well as natural resins. ATEC is used as a fixative for perfumes and as a plasticizer and film strengthening agent in hair sprays, nail polishes, and as an active ingredient in deodorants. Acetyl tributyl citrate is also commercialized as Citroflex<sup>®</sup> A-4 plasticizer. It is used widely in children's toys and food contact applications, and is an excellent plasticizer for vinyl toys. It can provide many improvements over di-butyl phthalate in cellulose nitrate films, including lower volatility, better adhesion to metals, and better resistance to yellowing [27]. To date, this environmentally friendly plasticizer has been prepared mainly by two methods: the direct esterification of triethyl citrate (TEC) with acetic acid [28] and the acetylation of TEC with acetic anhydride [29].

Zeolites have well-defined structures with microporous crystalline solids. Generally they are composed of silicon, aluminum, and oxygen in their framework and cations. They have been applying in many fields of catalysis, generating intense interest in these materials in industrial and academic laboratories. They present appreciable acid activity with shape-selective features as catalysts [30,31]. They have been adopted in various reactions as a heterogeneous catalyst [32]. However, acetylation of TEC for production of ATEC has not been employed on the zeolites catalysts for the production of ATEC.

This paper reports the preparation of ATEC by the acetylation of TEC with acetic anhydride on a range of acid catalysts. Microporous zeolites were introduced as a heterogeneous catalyst in the acetylation. This paper suggests a highly efficient catalyst for acetylation for the ATEC synthesis. The catalytic activities of the acid catalysts were estimated in comparison with the conversion of TEC and the selectivity of ATEC. The influences of the acid properties of HZSM-5 zeolite were evaluated and the catalytic activities in the acetylation reaction were compared.

## 2. Results and Discussion

### 2.1. Physicochemical Properties of the Zeolites

The  $\text{H}^+$  ion-exchanged zeolites (ZSM-5 and Y) are denoted as HZ and HY with their Si/Al molar ratios marked in the parentheses following the name such as HZ(25) and HY(3). Figure 1 presents X-ray diffraction (XRD) patterns and  $\text{N}_2$  isotherms of ZSM-5 and Y zeolites; they were identical to those published elsewhere [33]. The zeolites were highly crystalline. The  $\text{N}_2$  isotherms of HZ(25) showed the typical Langmuir-type isotherm. The large adsorption on HY(3) was caused by their large void fraction [34]. Figure 2 presents scanning electron microscopy (SEM) images of the zeolites. The particle sizes measured from the SEM images of ZSM-5 and Y zeolites were approximately  $0.5\text{ }\mu\text{m}$ .

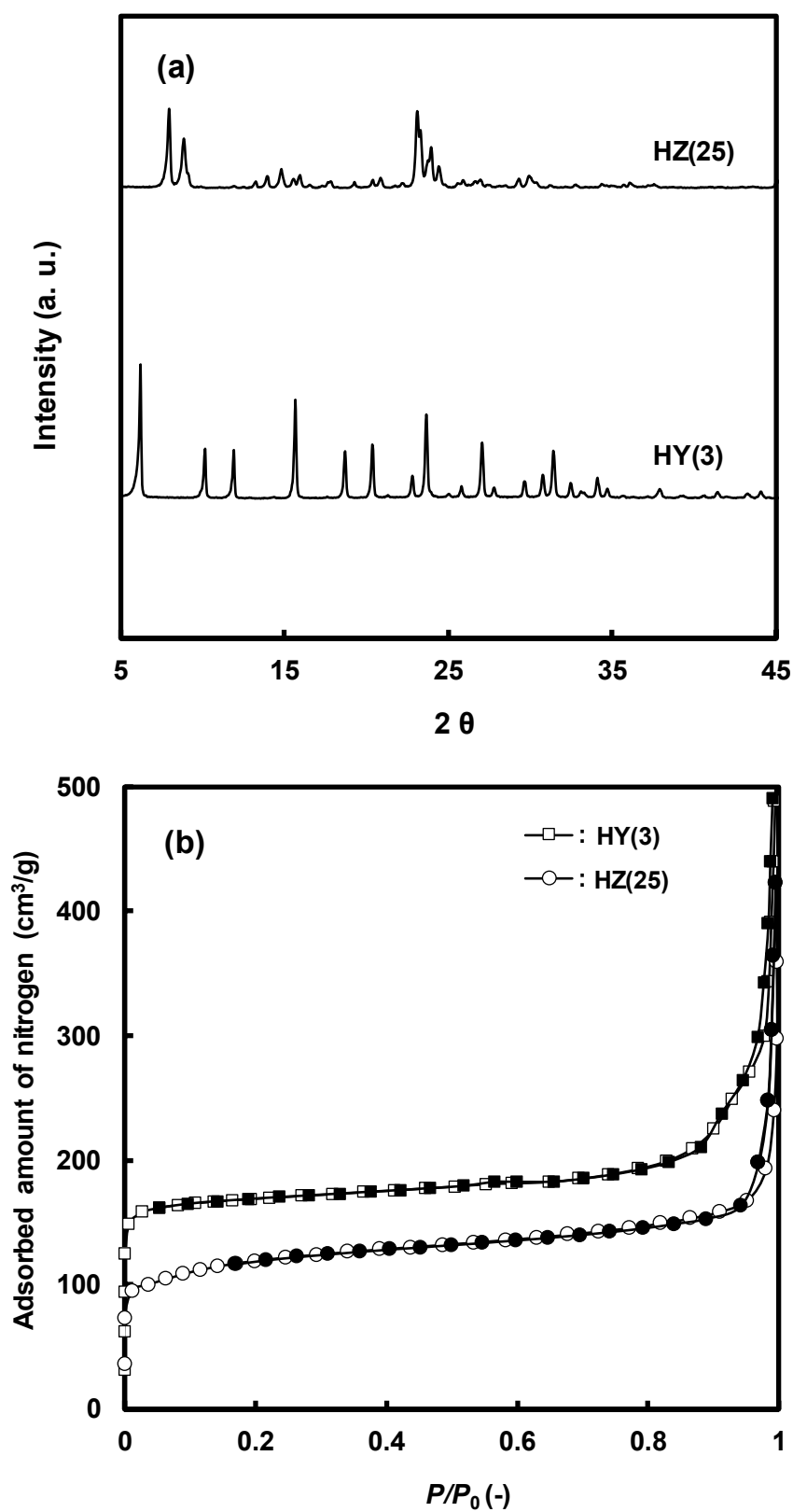
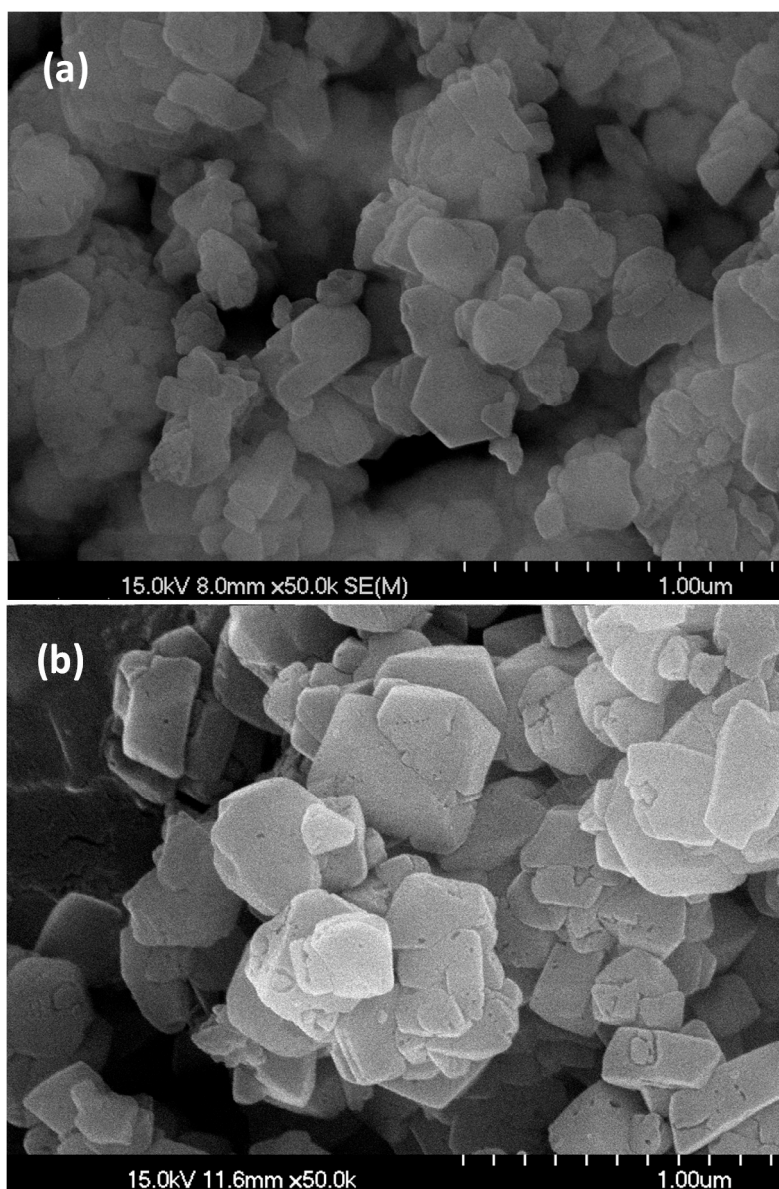
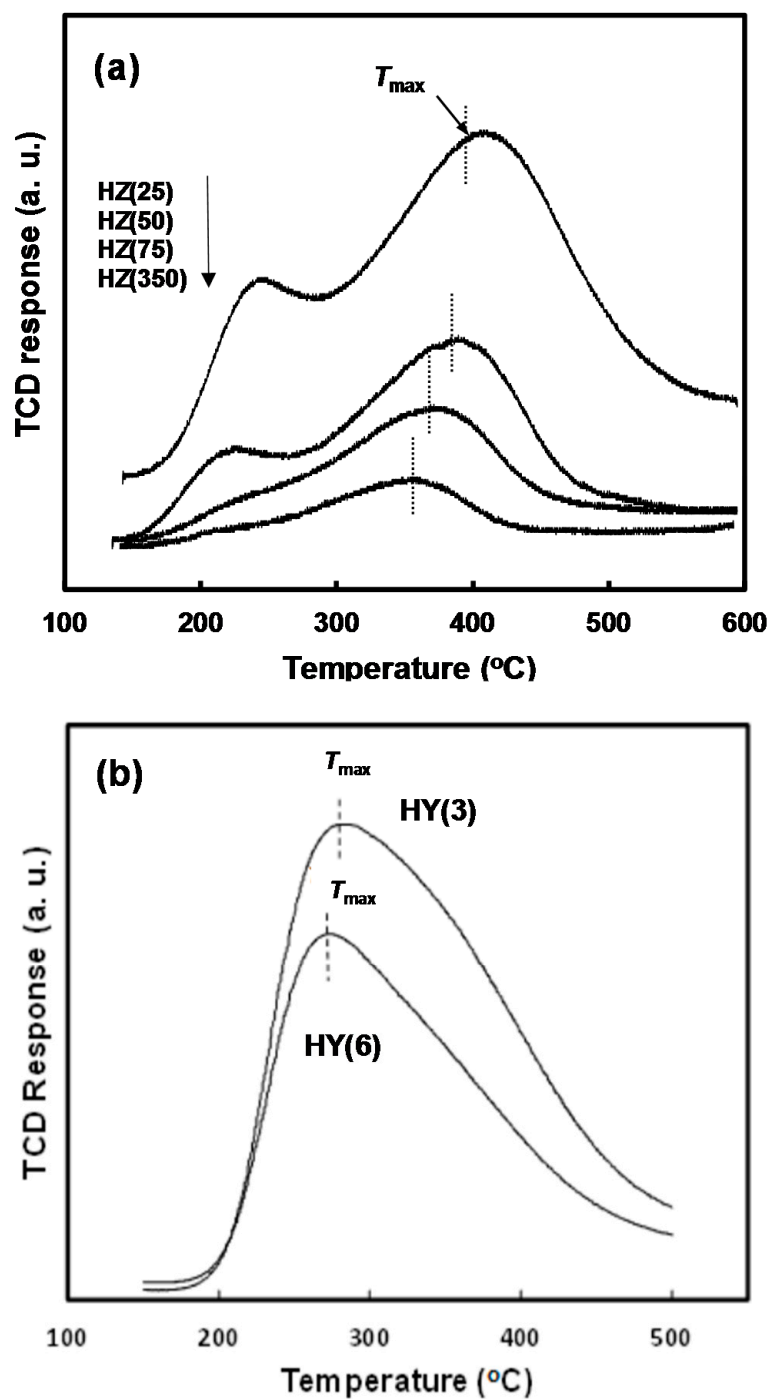


Figure 1. X-ray diffraction (XRD) patterns (a) and N<sub>2</sub> isotherms (b) of the zeolites.



**Figure 2.** Scanning electron microscopy (SEM) images of (a) HZ(25) and (b) HY(3) zeolites.

Zeolites have various acidic properties according to the species of zeolites. In addition, the acidic properties also change according to the Si/Al molar ratios. Ammonia temperature-programmed desorption ( $\text{NH}_3$ -TPD) measurements are performed to define the acidity of the catalysts (Figure 3). The number of acid sites of the catalysts was estimated from the area of the desorption peak. The acid strength was also determined from the temperature of maximum peak ( $T_{\text{max}}$ ) of the desorption peak concerned with the activation energy for ammonia desorption [35]. In general, the desorption peaks ranging from 350 °C to 550 °C are due to strong acid sites; on the other side, the peak of the weak acid sites or physically-adsorbed ammonia appeared at 150~250 °C [36]. The number of acid sites is reduced with decreasing Al content in the zeolite framework.



**Figure 3.** Ammonia temperature-programmed desorption (NH<sub>3</sub>-TPD) profiles of (a) H<sup>+</sup> ion-exchanged ZSM-5 (HZ) zeolites and (b) H<sup>+</sup> ion-exchanged Y (HY) zeolites with various Si/Al molar ratios.

Table 1 lists the physicochemical properties of the zeolites. Surface areas of the zeolites are summarized in the table. HY zeolites, which have a wide pore entrance and supercages in their framework, exhibited a wide surface area compared with those of HZSM-5 zeolites. The number of acid sites and  $T_{\max}$  obtained from the NH<sub>3</sub>-TPD results of the HY and HZ zeolites are also listed. The number of acid sites of the zeolites decreased with increasing Si/Al molar ratio. The  $T_{\max}$  values of the zeolites also decreased slightly with increasing Si/Al molar ratio.

**Table 1.** Physical and acidic properties of the zeolite catalysts.

Zeolite	Pore Topology	Pore Size (Å)	BET Surface Area (m <sup>2</sup> /g)	Acid Amount <sup>a</sup> (mmol/g)	T <sub>max</sub> <sup>b</sup> (°C)
HZ(25)	10-oxygen ring	5.1 × 5.6 [100] 6.3 × 5.6 [010]	413	7.9 × 10 <sup>−2</sup>	415
HZ(50)			405	4.5 × 10 <sup>−2</sup>	395
HZ(75)			407	3.8 × 10 <sup>−2</sup>	375
HZ(350)			418	0.5 × 10 <sup>−2</sup>	360
HY(3)	12-oxygen ring	7.4 × 7.4 [111]	574	9.1 × 10 <sup>−2</sup>	300
HY(6)			571	8.5 × 10 <sup>−2</sup>	280

<sup>a</sup> The value determined by deconvolution of NH<sub>3</sub>-TPD spectra from 250 °C to 600 °C; <sup>b</sup> The value determined from NH<sub>3</sub>-TPD spectra.

Figure 4 presents the FT-IR spectra of the zeolites adsorbed pyridine in the pretreatment process. The Brönsted acid sites can be defined from the band of pyridine adsorption. In the FT-IR spectra, the pyridine band at 1515–1565 cm<sup>−1</sup> was assigned to the Brönsted acid sites, and the band ranged in 1435–1470 cm<sup>−1</sup> corresponds to pyridine desorption coordinated to the Lewis acid sites. The band at 1545 cm<sup>−1</sup>, indicating the Brönsted acid sites, appeared on the HZ(25) zeolites. On the other hand, HY(3) zeolite showed a relatively intensive band at 1455 cm<sup>−1</sup>. The coefficients of B/L ratios of HZ(25) and HY(3), which were determined by Emeis method [37], were 17.7 and 1.6, respectively. The B/L coefficient of HZ(25) is higher than HY(3). This indicates that high catalytic activities of HZ(25) are caused by many Brönsted acid sites.

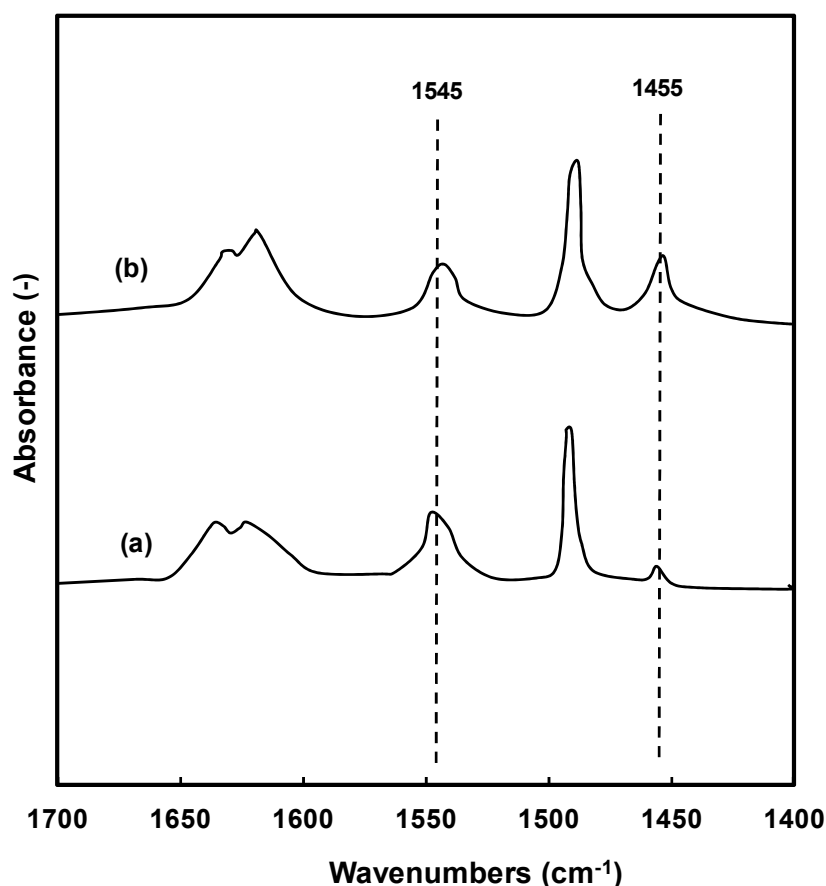


**Figure 4.** FT-IR spectra of pyridine adsorbed on the (a) HZ(25) and (b) HY(3) zeolites at room temperature and desorbed at 150 °C.

## 2.2. Catalytic Properties of the Zeolites in the Acetylation

The reaction pathway of the acetylation of TEC for formation of ATEC is presented in Figure 5. In the acetylation, the ATEC was produced mainly. Water was formed as a byproduct, and a little amount of acetic acid was observed. The conversion of the TEC was determined as the percentage of TEC consumed. The yield of ATEC is defined as its percentage to the summation of the products and reactants remaining. The selectivity of the ATEC was determined from the percentage of ATEC produced from the summation of the total products excluding water.

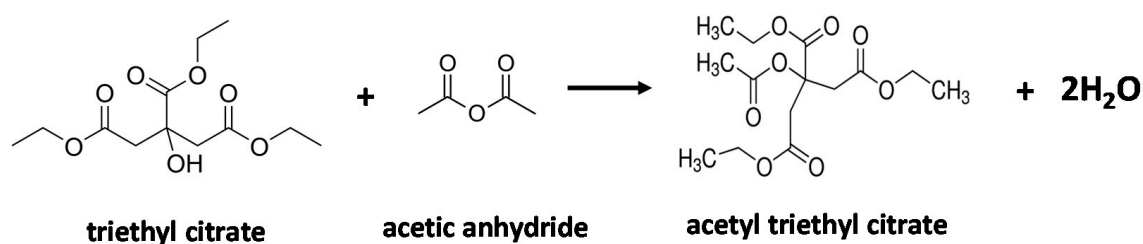


Figure 5. Reaction pathway of the acetylation of triethyl citrate (TEC) with acetic anhydride.

Figure 6 presents the catalytic activities of the HZ(50) zeolite with different loadings of zeolite catalyst. The conversions of TEC were improved according to the increase in catalysts loading. The selectivity of ATEC also increased with increasing catalysts loading. The selectivity approached ca. 100% at a >0.5 g catalyst loading after 1 h reaction time. Based on these results, the catalyst loading was determined as 0.5 g.

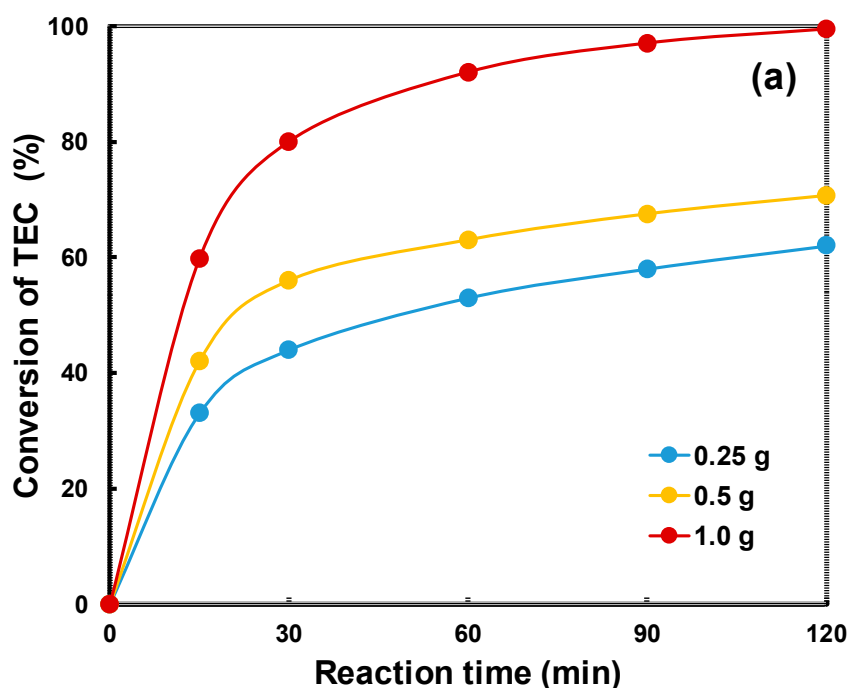
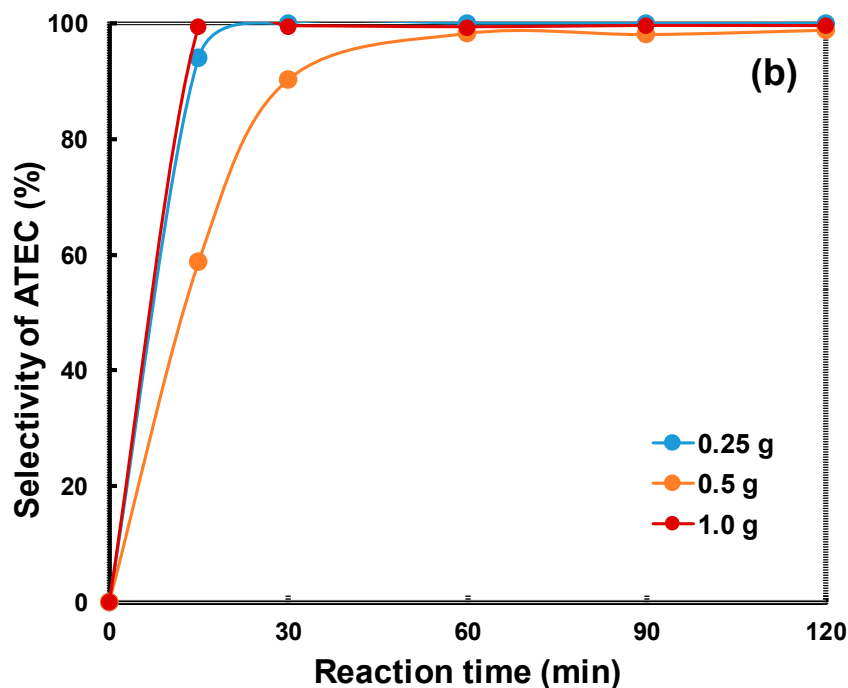


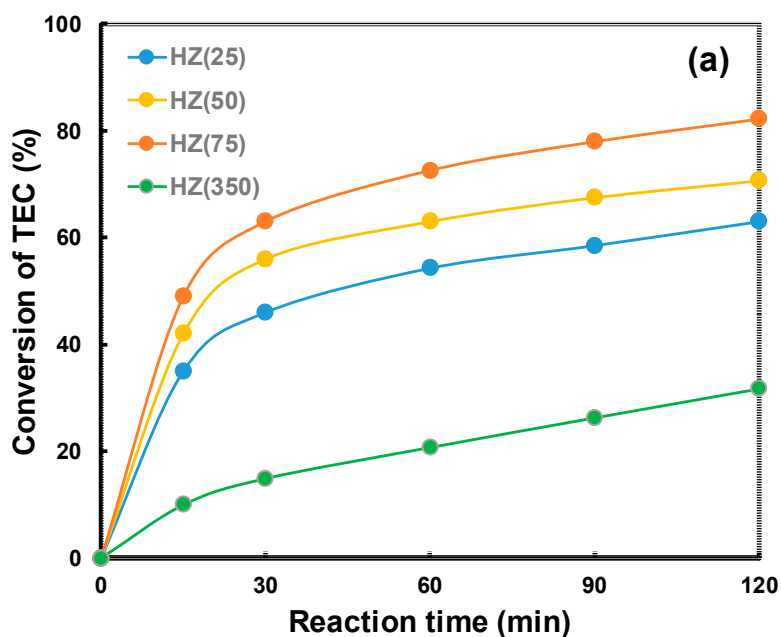
Figure 6. Cont.





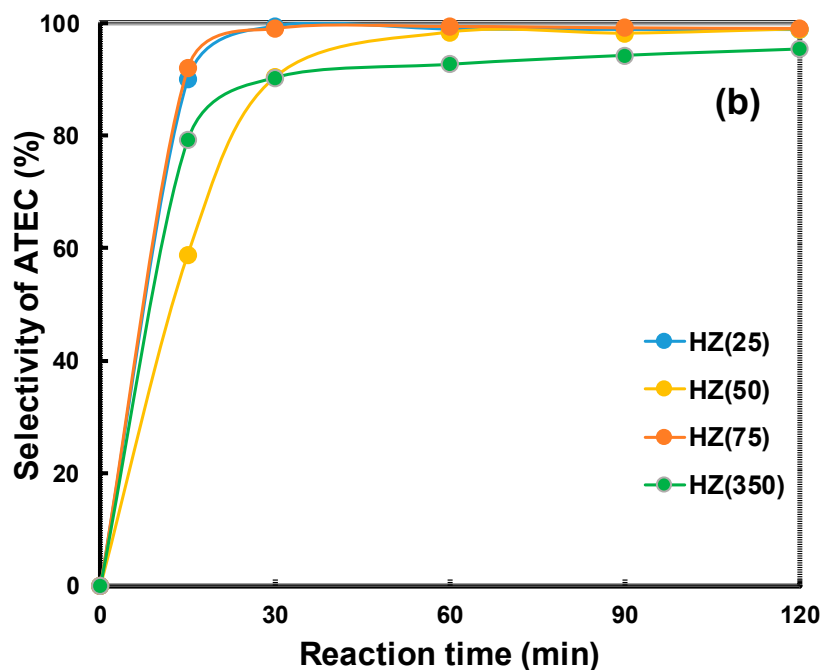
**Figure 6.** Conversion of TEC (a) and selectivity of acetyl triethyl citrate (ATEC) (b) in the acetylation over HZ(50) zeolite with different amount of catalyst loading.

Figure 7 presents the catalytic activities of HZSM-5 zeolite catalysts with various Si/Al molar ratios. The highest catalytic activity was observed on the HZ(75) zeolite among the HZSM-5 zeolite catalysts. The selectivity of ATEC on the HZ(25) and HZ(75) zeolite catalysts were similar, but the conversion was higher on HZ(75) zeolite than that on HZ(25) zeolite. In addition, HZ(350) zeolite, which has a weak acid strength, showed a low conversion compared to those of the other HZ zeolite catalysts. This indicates that an acid strength of catalysts is necessary to perform the catalytic reaction. However, it seems that a strong acidity is not able to lead a high selectivity of ATEC.



**Figure 7.** Cont.





**Figure 7.** Conversion of TEC (a) and selectivity of ATEC (b) in the acetylation over HZSM-5 zeolites with various Si/Al molar ratios.

Figure 8 shows the catalytic activities of HY zeolite with various Si/Al molar ratios in the acetylation of TEC after a 30 min reaction time. The selectivity of ATEC were greater than 90% on both HY(3) and HY(6) zeolite catalysts. On the other hand, conversions of TEC of them were nothing but 20%. Table 2 lists the catalytic activities of the various acid catalysts in the acetylation reaction. The catalytic activities of the HZSM-5 zeolite catalysts were superior to those of the HY zeolite catalysts. The selectivities of HY zeolite catalysts are high, but conversions of TEC are very low compared with those of HZSM-5 zeolite catalysts. It means that the selectivity of TEC depends on the pore properties of the zeolite catalysts. On the contrary, the conversion of TEC is affected on acid properties of the zeolite catalysts.

**Table 2.** Catalytic activities of the acid catalysts in the acetylation of TEC.

Catalysts	Conversion of TEC (%)	Selectivity of ATEC (%)
HZ(25)	63.0	98.8
HZ(50)	70.7	98.9
HZ(75)	82.2	99.1
HZ(350)	31.7	95.4
HY(3)	19.6	92.3
HY(6)	22.7	93.5

Figure 9 shows the dependence of the catalytic activities on the acid strength in the acetylation reaction on the HZSM-5 zeolites with various acid strengths. The highest catalytic properties were observed on HZ(75) zeolite. Although the acid strength was enhanced, the catalytic activities were lower on the HZ(25) and HZ(50) zeolites. The catalytic activities were lower on HZ(350) zeolite, which has very low acid strength. Therefore, a moderate acid strength led to high catalytic properties in acetylation for the preparation of ATEC.

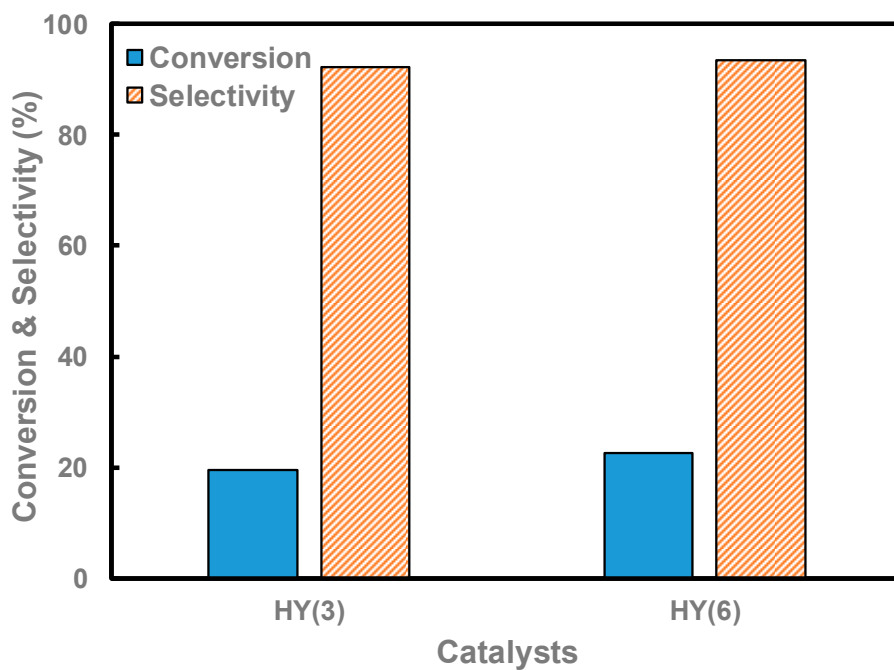


Figure 8. Conversion of TEC and selectivity of ATEC in the acetylation over HY zeolites of 1 h reaction time.

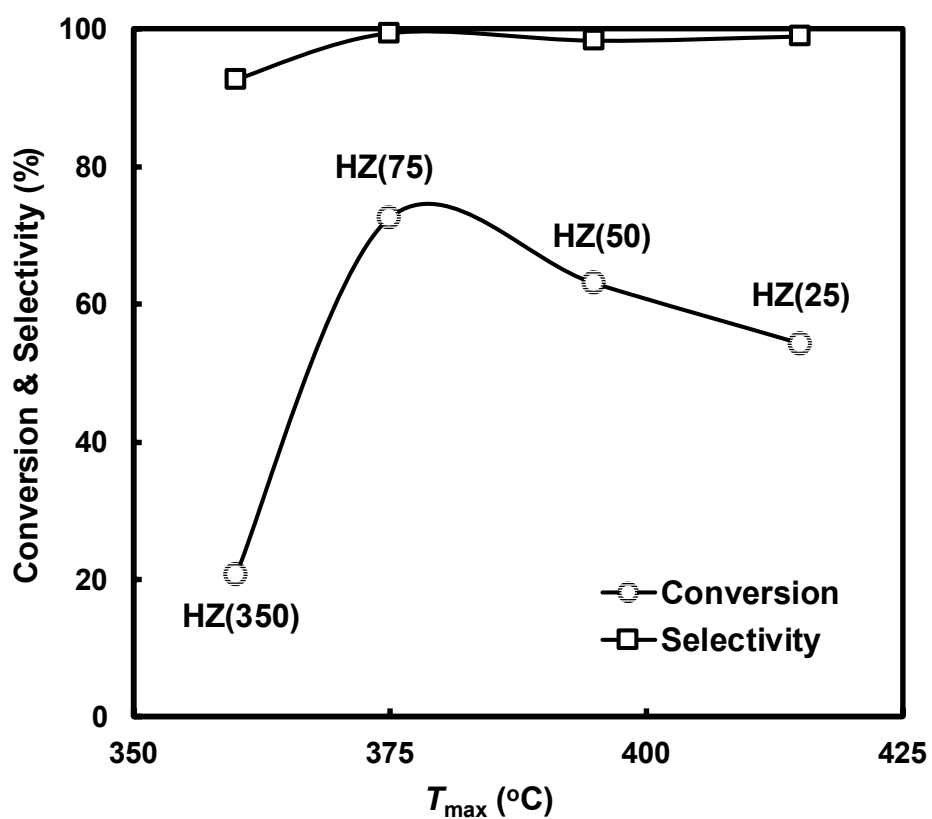


Figure 9. Dependence of catalytic activities of the HZSM-5 zeolite to their acid strength in the acetylation reaction.

### 3. Materials and Methods

#### 3.1. Catalysts

ZSM-5 zeolites were prepared through the hydrothermal synthesis of a synthetic mixture with different Si/Al molar ratios. The synthetic raw materials consisted of colloidal silica (40 wt % SiO<sub>2</sub>, Sigma-Aldrich, St. Louis, MO, USA), aluminum hydroxide (99%, Duksan, Seoul, Korea), potassium hydroxide (99%, Duksan, Seoul, Korea), and deionized water. Synthesis by the thermal reaction was carried out by aging for 48 h and heating at 180 °C for 24 h. The Si/Al molar ratio of the synthesized ZSM-5 zeolites was defined as 50 and 350, respectively. Other ZSM-5 zeolites with various Si/Al molar ratios were purchased from Zeolyst Co. (Kansas City, MO, USA).

The Na-type ZSM-5 zeolite was treated with a 0.5 N ammonium nitrate solution (Daejung, 99%) at 70 °C to exchange their cations to ammonium ions. The H<sup>+</sup> ion-exchanged ZSM-5 (HZ) zeolite was prepared by calcination at 500 °C for 5 h. The Y zeolites were purchased from Tosoh Co. (Tokyo, Japan) with various Si/Al molar ratios. The H<sup>+</sup> ion-exchanged Y zeolites (HY) were prepared using the method mentioned above. The prepared H-form zeolites are denoted as HZ and HY with their Si/Al molar ratios marked in the parentheses following the name such as HZ(25) and HY(3).

#### 3.2. Characterization of Physicochemical Properties of the Zeolite

XRD (Rigaku D/MAX-2500/PC, Tokyo, Japan) of the zeolites was performed using nickel filtered Cu K $\alpha$  X-rays at 40 kV and 40 mA with a scan rate of 2°/min. The morphology and particle size of the zeolites were estimated by SEM (Hitachi, S-4700, Tokyo, Japan). Their Si and Al composition were determined from the results using an energy dispersive X-ray attachment (EDS; NORAN, Z-MAX 300, Tokyo, Japan). The N<sub>2</sub> isotherms were measured using an automatic volumetric adsorption system (MSI, Porosity-XQ, Gwangju, Korea) at the temperature of liquid nitrogen. Evacuation of the samples was carried out at 130 °C for 1 h before nitrogen adsorption.

The NH<sub>3</sub> temperature programmed desorption (NH<sub>3</sub>-TPD) profiles of the zeolites were measured using a chemisorption analysis instrument (Bel Japan, Belsorp, Osaka, Japan). A pretreatment was performed through activation in flowing helium at 500 °C for 2 h, followed by cooling to 130 °C. Ammonia gas was injected into the samples in pulses until saturation was reached. The saturated samples were then purged by helium flow at 150 °C for 2 h to remove the adsorbed ammonia physically. The temperature of the sample was heated to 600 °C at a 10 °C/min ramping rate. The number of strong acid sites was estimated by the peak deconvolution of the measured spectra from 250 °C to 600 °C.

The Fourier transform infrared (FT-IR; Bomem, MB155, Quebec, QC, Canada) spectra were measured using self-supported wafers of 10 mg/cm<sup>2</sup>. The samples were evacuated at 180 °C for 6 h in a 10<sup>−3</sup> Pa dynamic vacuum for 12 h. Pyridine was then injected into the cell. The samples were evacuated at 130 °C under vacuum and cooled to room temperature. The FT-IR spectra were then recorded.

#### 3.3. Acetylation of TEC with Acetic Anhydride

The acetylation of TEC with acetic anhydride over various acid catalysts was carried out by stirring magnetically in a glass reactor equipped with a cooling condenser. TEC (99%, Sigma-Aldrich, St. Louis, MO, USA) and acetic anhydride (99%, Duksan, Seoul, Korea) were introduced as the reactants without further purification in the acetylation.

The reactants, TEC (0.2 mol) and acetic anhydride (0.25 mol), were introduced into the reactor with the catalyst. The amount of catalysts loaded in the acetylation was 0.25–1 g. The stirring speed was maintained at 500 rpm. The acetylation reaction was performed with stirring at 130 °C for 5 h. The composition of the products taken at regular time intervals was analyzed by gas chromatography (GC7A, Shimadzu, Tokyo, Japan) using a capillary column (DB-1, i.d.: 0.32 mm, film thickness: 0.17  $\mu$ m, length: 50 m) and a FID detector.

#### 4. Conclusions

ATEC was prepared by the acetylation of TEC with acetic anhydride on various zeolite catalysts. The catalytic activities of the zeolite catalysts were estimated by a comparison with the conversion of TEC and the selectivity of ATEC. The HZSM-5 zeolite catalysts showed high conversion of TEC and excellent selectivity of ATEC. HZ(75) zeolite was found to be a highly efficient catalyst in the acetylation for ATEC synthesis. In particular, the selectivity of ATEC on the HZ(75) zeolites exceeded 95%. The high catalytic activities of HZ(25) are caused by many Brönsted acid sites. This suggests that the moderate acid strength of HZ(75) zeolite led to the highest catalytic activities among the HZSM-5 zeolites with various acid strengths.

**Acknowledgments:** This research was supported by the Civil research projects for solving social problems through the National Research Foundation of Korea (NRF) funded by the Ministry of Science, ICT & Future Planning (2015M3C8A6A06012988).

**Author Contributions:** K.-H.C. and Sangmin J. conceived and designed the experiments; K.-H.C. and Sangmin J. performed the experiments; H.K. and S.-J.K. analyzed the data; K.-H.C. and S.-C.J. wrote the paper; and Y.-W.P. revised the paper.

**Conflicts of Interest:** The authors declare no conflict of interest.

#### References

1. Sang, B.; Li, Z.; Yu, L.; Li, X.; Zhang, Z. Preparation of zinc hydroxystannate-titanate nanotube flame retardant and evaluation its smoke suppression efficiency for flexible polyvinyl chloride matrix. *Mater. Lett.* **2017**, *204*, 133–137. [[CrossRef](#)]
2. Lu, J.; Liu, X.; Wang, Y.; Lin, J.; Peng, N.; Li, J.; Zhao, F. Performance enhancement of polyvinyl chloride ultrafiltration membrane modified with graphene oxide. *J. Colloid Interface Sci.* **2016**, *480*, 1–8.
3. Hunge, Y.M.; Mahadik, M.A.; Moholkar, A.V.; Bhosale, C.H. Photoelectrocatalytic degradation of *phthalic acid* using spray deposited stratified WO<sub>3</sub>/ZnO thin films under sunlight illumination. *Appl. Surf. Sci.* **2017**, *420*, 764–772. [[CrossRef](#)]
4. Sandhwar, V.K.; Prasad, B. Comparison of *phthalic acid* removal from aqueous solution by electrochemical methods: Optimization, kinetic and sludge study. *J. Environ. Manag.* **2017**, *203*, 476–488. [[CrossRef](#)] [[PubMed](#)]
5. Rahman, M.; Brazel, C. The Plasticizer Market: An Assessment of Traditional Plasticizers and Research Trends to Meet New Challenges. *Prog. Polym. Sci.* **2004**, *29*, 1223–1248. [[CrossRef](#)]
6. Wypych, G. *Plasticizer Types Handbook of Plasticizers*; Chem Tec Publishing: Toronto, ON, USA, 2000; pp. 7–71.
7. Pan, H.; Hao, Y.; Lang, X.; Zhang, Y.; Wang, Z.; Zhang, H.; Dong, L. Improved mechanical properties, barrier properties and degradation behavior of poly(butylene adipate-coterephthalate)/poly(propylene carbonate) films. *Korean J. Chem. Eng.* **2017**, *34*, 1294–1304. [[CrossRef](#)]
8. Heudorf, U.; Mersch-Sundermann, V.; Angerer, J. Phthalates: Toxicology and Exposure. *Int. J. Hyg. Environ. Health* **2007**, *210*, 623–634. [[CrossRef](#)] [[PubMed](#)]
9. Saillenfait, A.-M.; Laudet-Hesbert, A. Phthalates (II). *EMC Toxicol.* **2005**, *2*, 137–150. [[CrossRef](#)]
10. Van Haveren, J.; Oostveen, E.A.; Micciché, F.; Weijnen, J.G.J. How biobased products contribute to the establishment of sustainable, phthalate free, plasticizers and coatings. In *Feedstocks for the Future*; Bozell, J.J., Patel, M.K., Eds.; American Chemical Society: Washington, DC, USA, 2006; pp. 99–115.
11. Wilkinson, C.F.; Lamb, J.C. The potential health effects of phthalate esters in children's toys: A review and risk assessment. *Regul. Toxicol. Pharmacol.* **1999**, *30*, 140–155. [[CrossRef](#)] [[PubMed](#)]
12. Kawakami, T.; Isama, K.; Matsuoka, A. Analysis of phthalic acid diesters, monoester, and other plasticizers in polyvinyl chloride household products in Japan. *J. Environ. Sci. Health Part A Toxic Hazard. Subst. Environ. Eng.* **2011**, *46*, 855–864. [[CrossRef](#)] [[PubMed](#)]
13. Dias, C.R.; Portela, M.F.; Bond, G.C. Synthesis of phthalic anhydride: Catalysts, Kinetics, and Reaction Modeling. *Catal. Rev.* **1997**, *39*, 169–207. [[CrossRef](#)]
14. Reinecke, H.; Navarro, R.; Pérez, M. Plasticizers. In *Handbook of Polymer Science and Technology*; John Wiley & Sons, Inc.: New York, NY, USA, 2011; pp. 1–27.

15. Kolah, A.K.; Asthana, N.S.; Vu, D.T.; Lira, C.T.; Miller, D.J. Reaction Kinetics of the Catalytic Esterification of Citric Acid with Ethanol. *Ind. Eng. Chem. Res.* **2007**, *46*, 3180–3187. [CrossRef]
16. Arendt, W.D.; Joshi, M. *Specialty Plasticizers Handbook of Vinyl Formulating*; John Wiley & Sons, Inc.: New York, NY, USA, 2008; pp. 239–286.
17. Miller, D.J.; Asthana, N.; Kolah, A.; Vu, D.T.; Lira, C.T. Process for Reactive Esterification Distillation. U.S. Patent 7667068 B2, 23 February 2010.
18. Schröter, J.; Konetzke, G.; Weidemann, F.; Klein, T.; Bohnen, H.; Bergrath, K.; Schmidt, K. Method for Producing Citric Acid Esters. WO2003008369, 30 January 2003.
19. Bohnen, H.; Bergrath, K.; Klein, T. Citric Esters and a Process for Their Preparation. U.S. Patent 2002/0198402 A1, 8 May 2002.
20. Kolah, A.K.; Asthana, N.S.; Vu, D.T.; Lira, C.T.; Miller, D.J. Triethyl Citrate Synthesis by Reactive Distillation. *Ind. Eng. Chem. Res.* **2008**, *47*, 1017–1025. [CrossRef]
21. Verhoff, F.H. *Citric Acid. Ullmann's Encyclopedia of Industrial Chemistry*; Wiley-VCH Verlag GmbH & Co KGaA: Weinheim, Germany, 2005; p. 69.
22. Osorio-Pascuas, O.M.; Santaella, M.A.; Rodriguez, G.; Orjuela, A. Esterification Kinetics of Tributyl Citrate Production Using Homogeneous and Heterogeneous Catalysts. *Ind. Eng. Chem. Res.* **2015**, *54*, 12534–12542. [CrossRef]
23. Jia, P.; Hu, L.; Feng, G.; Bo, C.; Zhou, Y. PVC materials without migration obtained by chemical modification of azide-functionalized PVC and triethyl citrate plasticizer. *Mater. Chem. Phys.* **2017**, *190*, 25–30. [CrossRef]
24. Finkelstein, M.; Gold, H. Toxicology of the citric acid esters: Tributyl citrate, acetyl tributyl citrate, triethyl citrate, and acetyl triethyl citrate. *Toxicol. Appl. Pharmacol.* **1959**, *1*, 283–298. [CrossRef]
25. Sawada, S.; Ursino, C.; Galiano, F.; Simone, S.; Figoli, A. Effect of citrate-based non-toxic solvents on poly(vinylidene fluoride) membrane preparation via thermally induced phase separation. *J. Membr. Sci.* **2015**, *493*, 232–242. [CrossRef]
26. Pang, C.; Shanks, R.A.; Daver, F. Characterization of kenaf fiber composites prepared with tributyl citrate plasticized cellulose acetate. *Compos. Part A Appl. Sci. Manuf.* **2015**, *70*, 52–58. [CrossRef]
27. Vertellus. Available online: <http://www.vertellus.com> (accessed on 24 October 2017).
28. Sakakura, A.; Nakagawa, S.; Ishihara, K. Direct ester condensation catalyzed by bulky diarylammonium pentafluorobenzenesulfonates. *Nat. Protocol.* **2007**, *2*, 1746–1751. [CrossRef] [PubMed]
29. Sakakura, A.; Kawajiri, K.; Ohkubo, T.; Kosugi, Y.; Ishihara, K. Widely useful DMAP-catalyzed esterification under auxiliary base- and solvent-free conditions. *J. Am. Chem. Soc.* **2007**, *129*, 14775–14779. [CrossRef] [PubMed]
30. Jeong, J.M.; Park, J.H.; Baek, J.H.; Hwang, R.H.; Jeon, S.G.; Yi, K.B. Effects of acid treatment of Fe-BEA zeolite on catalytic N<sub>2</sub>O conversion. *Korean J. Chem. Eng.* **2017**, *34*, 81–86. [CrossRef]
31. Davoodpour, M.; Tafreshi, R.; Khodadadi, A.A.; Mortazavi, Y. Two-stage cracking catalyst of amorphous silica-alumina on Y zeolite for enhanced product selectivity and suppressed coking. *Korean J. Chem. Eng.* **2017**, *34*, 681–691. [CrossRef]
32. Suppes, G.J.; Dasari, M.A.; Doskocil, E.J.; Mankidy, P.J.; Goff, M.J. Transesterification of soybean oil with zeolite and metal catalysts. *Appl. Catal. A Gen.* **2004**, *257*, 213–223. [CrossRef]
33. Robeson, H.; Lillerud, K.P. *Verified Synthesis of Zeolitic Materials*, 2nd ed.; Elsevier: Amsterdam, The Netherlands, 2001; pp. 225–227.
34. Thommes, M.; Kaneko, K.; Neimark, A.V.; Olivier, J.P.; Rodriguez-Reinoso, J.; Rouquerol, J.; Sing, K.S.W. Physisorption of gases, with special reference to the evaluation of surface area and pore size distribution (IUPAC Technical Report). *Pure Appl. Chem.* **2015**, *87*, 1051–1069. [CrossRef]
35. Kadata, N.; Igi, H.; Kim, J.-H.; Niwa, M. Determination of the acidic properties of zeolite by theoretical analysis of temperature-programmed desorption of ammonia based on adsorption equilibrium. *J. Phys. Chem. B* **1997**, *101*, 5969–5977. [CrossRef]
36. Niwa, M.; Kadata, N.; Sawa, M.; Murakami, Y. Temperature-programmed desorption of ammonia with readsorption based on the derived theoretical equation. *J. Phys. Chem. B* **1995**, *99*, 8812–8816. [CrossRef]
37. Emeis, C.A. Determination of integrated molar extinction coefficients for infrared absorption bands of pyridine adsorbed on solid acid catalysts. *J. Catal.* **1993**, *141*, 347–354. [CrossRef]



© 2017 by the authors. Licensee MDPI, Basel, Switzerland. This article is an open access article distributed under the terms and conditions of the Creative Commons Attribution (CC BY) license (<http://creativecommons.org/licenses/by/4.0/>).